Sub-Doppler laser cooling and magnetic trapping of erbium

Andrew J. Berglund,[1] Siu Au Lee,[2] and Jabez J. McClelland[1]
[1]*Center for Nanoscale Science and Technology, National Institute of Standards and Technology, Gaithersburg, Maryland 20899, USA*
[2]*Department of Physics, Colorado State University, Ft. Collins, Colorado 80534, USA*
(Received 22 June 2007; revised manuscript received 17 September 2007; published 27 November 2007)

We investigate cooling mechanisms in magneto-optically and magnetically trapped erbium. We find efficient sub-Doppler cooling in our trap, which can persist even in large magnetic fields due to the near degeneracy of two Landé g factors. Furthermore, a continuously loaded magnetic trap is demonstrated where we observe temperatures below 25 μK. These favorable cooling and trapping properties suggest a number of scientific possibilities for rare-earth-metal atomic physics, including narrow linewidth laser cooling and spectroscopy, unique collision studies, and degenerate bosonic and fermionic gases with long-range magnetic dipole coupling.

DOI: 10.1103/PhysRevA.76.053418 PACS number(s): 32.80.Pj

I. INTRODUCTION

The maturation of laser-cooling and trapping techniques has enabled many recent advances with elements ranging over much of the periodic table. Narrow intercombination lines in Sr provide ultraprecise atomic frequency standards [1,2]; Yb has also been proposed as a frequency standard [3,4], with quantum degeneracy recently reached in both bosonic [5] and fermionic isotopes [6]; a Ra magneto-optical trap (MOT) promises new tests of fundamental symmetries, while also exhibiting an interesting black-body radiation repumping mechanism [7]; Cr has a large ground-state magnetic moment ($6\mu_B$), which is expected to give long-range order to a Bose-Einstein condensate [8]. In an extension of laser-cooling techniques to a highly magnetic rare-earth-metal atom, one of us recently reported an Er MOT where a novel recycling mechanism allows trapping despite significant leakage into energy levels that are dark to the cooling light [9].

Along with the other rare-earth-metal elements, erbium offers an exciting combination of favorable properties for future cold atomic physics experiments. All six stable isotopes have been trapped, with significant populations in three bosonic (^{166}Er, ^{168}Er, ^{170}Er) and one fermionic (^{167}Er, nuclear spin $I=7/2$) species. Er exhibits a variety of accessible transitions that are useful for spectroscopy or laser cooling, including a broad (36 MHz) line at 401 nm, a narrow (8 kHz) line at 841 nm, and an ultranarrow (2 Hz) line in the telecommunication spectrum at 1299 nm [10–12]. It has a very large ground-state magnetic moment ($7\mu_B$), which produces a strong magnetic dipole interaction at low temperatures. Its closed $5s^2$ and $6s^2$ electron shells shield the $4f$ core electrons, resulting in novel scattering properties while also suppressing undesirable Zeeman relaxation rates [13]. Additionally, a deterministic ion implantation source based on an Er MOT [14] could provide a single-ion analog of a solid-state laser while dramatically enhancing the prospects for scalability in recent rare-earth-metal quantum computing proposals [15]. However, none of these avenues can be pursued without first understanding the laser-cooling and trapping properties of this new system.

The primary result of this paper is an exhibition of cooling and trapping properties, both magnetic and optical, which bolster the growing list of erbium's desirable features for future cold atomic physics. First, we show that efficient sub-Doppler cooling occurs in our MOT where temperatures reach as low as 100 μK, nearly an order of magnitude below the Doppler temperature ($T_D=860$ μK). Second, we point out that for the 401 nm transition, the Landé g factors describing the Zeeman shift of the ground- and excited-state magnetic sublevels are nearly equal. This near degeneracy of Landé g should soften the usual constraint that $\sigma^+\sigma^-$ polarization gradient cooling can only occur in negligible magnetic fields and may have interesting applications for atomic beam collimation or atomic waveguiding along magnetic field lines. Finally, we show that a magnetically trapped atom fraction in our MOT is unexpectedly cold, with temperatures falling below 25 μK, lower than expectations based on simple thermodynamic considerations. We believe these magneto-optical properties, coupled with the unique atomic properties of the rare-earth-metal elements, make Er an exciting candidate for a wide range of future experiments.

II. SUB-DOPPLER COOLING IN THE MOT

Our apparatus was described in Ref. [9]. An effusive atomic beam is produced in the horizontal (x) direction by heating a sample of Er to 1200 °C in a crucible with a 1 mm aperture. The beam is subsequently decelerated in a σ^- Zeeman slower [16] then loaded into a MOT operating on the strong ($\Gamma/2\pi=36$ MHz) transition at 401 nm. Cooling and trapping light is derived from a frequency-doubled Ti:sapphire laser. The Zeeman slower beam, MOT beams, and a probe beam are derived from the same laser, with frequency offsets and relative intensities controlled by acousto-optic modulators. All laser frequencies are calibrated and locked to a fluorescence probe on the atomic beam, with an overall uncertainty of ±2.8 MHz [26]. The quadrupole magnetic field at the trap position is the sum of fields from our MOT coils together with the Zeeman slower and compensation coils, with the largest gradient along the direction of gravity (z). Typical field gradients are $(dB_x, dB_y, dB_z)=(0.20, 0.11, -0.33)$ T/m with ±5% uncertainty. All of the measurements described here were performed on ^{166}Er, with trapped atom populations between 10^4 and 2×10^5.

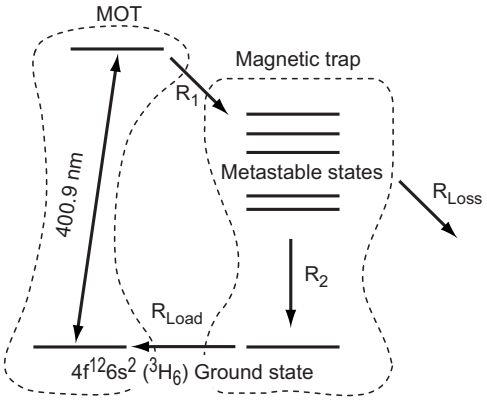

FIG. 1. Schematic level diagram of the Er MOT and magnetic trap [9]. The excited state of the 401 nm transition decays into magnetically trapped metastable states at a rate $R_1 \approx 1700\ \mathrm{s}^{-1}$. Relaxation to the ground state at rate R_2 and trap loss at rate R_{Loss} both occur with rates of 4 to 5 s^{-1}. R_{Load} varies depending on MOT conditions.

Er exhibits a complex level structure, with 110 electronic states lying between the ground and excited state of the 401 nm laser-cooling transition. As shown in Fig. 1, the MOT remains functional because decay of excited atoms into metastable intermediate states does not necessarily result in the loss of those atoms. On the contrary, a large fraction of these metastable, dark-state atoms remain magnetically trapped and eventually relax back to the ground state. We begin by studying the temperature of the MOT, which we measure by observing the ballistic expansion of the atom cloud after all optical and magnetic fields are extinguished. The cloud is imaged by pulsing the MOT beams for 200 μs and recording the resulting fluorescence image (in the xz plane) using a CCD camera. Figure 2 shows the measured temperature T as a function of the detuning of the MOT beams δ. The error bars represent uncertainty estimates from variation in the expansion velocity determined independently along the x and z directions. The upper solid curve shows the prediction of simple Doppler theory for a two-level atom [17], while the lower curve is a fit to a characteristic sub-Doppler scaling law [18,19]

$$T = T_0 + C_{\sigma^+\sigma^-}\frac{\hbar\Gamma}{2k_B}\left(\frac{\Gamma}{|\delta|}\right)\frac{I}{I_s}, \tag{1}$$

where I is the total intensity at the MOT position and $I_s = 72\ \mathrm{mW/cm^2}$ is the saturation intensity. The resulting fit gives $C_{\sigma^+\sigma^-}=0.38\pm0.02$ and a predicted minimum temperature $T_0=77\pm10\ \mu$K in the zero-intensity limit. We also varied the intensity at fixed detuning $\delta=-0.7\Gamma$ (inset of Fig. 2), to find $C_{\sigma^+\sigma^-}=0.15\pm0.08$ and $T_0=125\pm21\ \mu$K. The difference in fit parameters between the data sets indicates that the temperature may have a more complicated dependence on intensity than the simple scaling law of Eq. (1). This is not too surprising, since in our trap, intensity-dependent rates of optical pumping into magnetically trapped dark states may

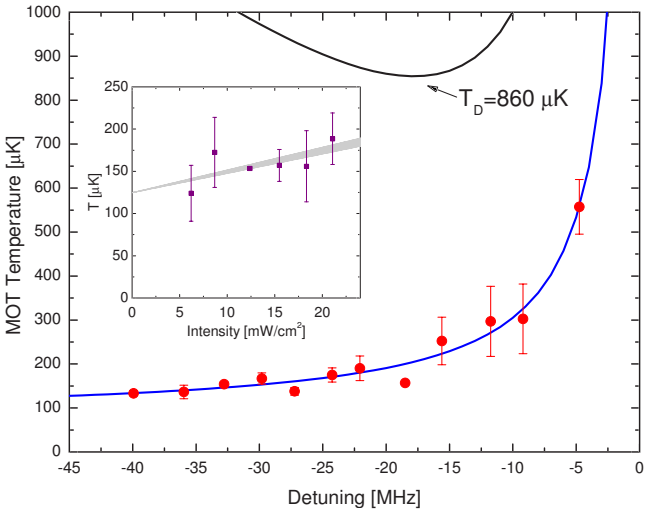

FIG. 2. (Color online) MOT temperature vs detuning for $I = 14.3\ \mathrm{mW/cm^2}$. The upper curve is expected for Doppler cooling a two-level atom, while the lower curve is a fit to Eq. (1). The atom number ranged from a minimum value of approximately 10^4 at $\delta/2\pi=-5$ MHz to a maximum of 1.3×10^5 at $\delta/2\pi=-30$ MHz (-0.8Γ). (Inset) MOT temperature vs trapping beam intensity at a fixed detuning $\delta=-0.7\Gamma$. The shaded gray area is a fit to Eq. (1) together with the spread resulting from uncertainty in δ. Error bars are described in the text.

strongly affect the MOT temperature (we show below that the magnetically trapped atom fraction exhibits anomalous temperature behavior). Nevertheless, our results show qualitatively and quantitatively that strong, efficient sub-Doppler cooling occurs in the MOT. We emphasize that this is a single-stage process (see also Ref. [19]), where sub-Doppler cooling occurs in the MOT without an additional "optical molasses" period of polarization-gradient cooling in a nulled magnetic field.

As discussed in Refs. [20,21], $\sigma^+\sigma^-$ polarization-gradient cooling typically breaks down in a longitudinal magnetic field because the "locking velocity," where atomic-motion-induced frequency shifts are balanced by Zeeman shifts, is generally different for sub-Doppler and Doppler cooling mechanisms. This difference arises because Doppler mechanisms rely on absorption and spontaneous emission, so Zeeman shifts of both the ground and excited states affect the cooling efficiency; on the other hand, sub-Doppler mechanisms rely on stimulated processes between ground-state sublevels, and thus depend primarily on Zeeman shifts in the ground state. Because the Landé g factors of the ground and excited states of a cooling transition are generally unequal, there is a critical magnetic field value at which the two mechanisms "unlock," with the larger capture range of the Doppler cooling force dominating beyond this point [20,21]. For most laser-cooled atoms, this critical magnetic field value is around 0.1 mT. In Xe, for example, the difference in g factors between the ground and excited state is $\Delta g_{eg} = -0.17$ and polarization-gradient cooling was observed to fail at 0.2 mT [22]. On the other hand, the g factor difference

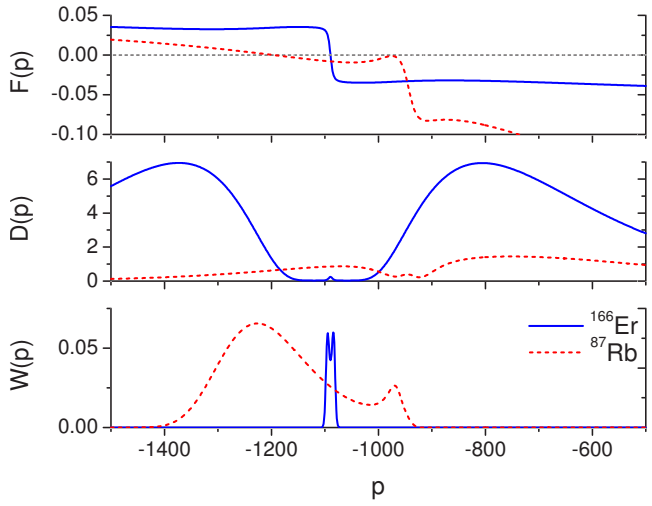

FIG. 3. (Color online) Semiclassical force $F(p)$ (in units of $\hbar k\Gamma$), momentum diffusion coefficient $D(p)$ (in units of $\hbar^2k^2\Gamma$), and equilibrium probability distribution $W(p)$ (arbitrary units) for ^{87}Rb (dashed lines, red) and ^{166}Er (solid lines, blue) in a $\sigma^+\sigma^-$ optical molasses in a longitudinal magnetic field $B=1$ mT. For both cases, the saturation parameter $s=2$ and detuning $\delta=-2.5\Gamma$.

for the 401 nm transition in Er is $\Delta g_{eg}=-0.004$ [10], suggesting that $\sigma^+\sigma^-$ polarization-gradient cooling should remain effective in longitudinal magnetic fields as large as 10 mT.

To investigate the possible effect of g factor degeneracy on Er sub-Doppler cooling in a magnetic field, we calculated the semiclassical force $F(p)$, momentum diffusion coefficient $D(p)$, and steady-state momentum distribution $W(p)$ for an atom with momentum $\hbar kp$ in a one-dimensional $\sigma^+\sigma^-$ optical molasses in a longitudinal magnetic field B. Our calculations follow the method of Ref. [20], in which p is treated as a classical variable and a Fokker-Planck equation is derived by expanding the optical Bloch equations to second order in $\hbar k$. Results are shown in Fig. 3 for the 401 nm line of ^{166}Er and for the D_2 line of ^{87}Rb ($\Delta g_{eg}=-0.17$) in a magnetic field $B=1$ mT. Because of the complicated interplay between optical coherences, Zeeman coherences, and atomic momentum, the distributions $W(p)$ are clearly not Gaussian. As a result, a temperature does not exist in the strict sense, but we may still take the variances of $W(p)$ as a measure of the momentum spread. These variances correspond to center-of-mass "temperatures" of 25 μK and 3.6 mK for ^{166}Er and ^{87}Rb, respectively. The same calculation gives respective temperatures of 25 and 17 μK at zero magnetic field $B=0$. For this simplified one-dimensional case, the g-factor difference results in a temperature increase of more than 2 orders of magnitude for ^{87}Rb, with no change in temperature for ^{166}Er, at a magnetic field value of $B=1$ mT (10 G). Note that this value of the magnetic field is attained in our setup at a distance of a few millimeters from the MOT position, within the beam waist of our trapping lasers. The near degeneracy of Er g factors may contribute to capture and loading processes in our MOT and should also have interesting applications for laser cooling Er in moderately large magnetic fields.

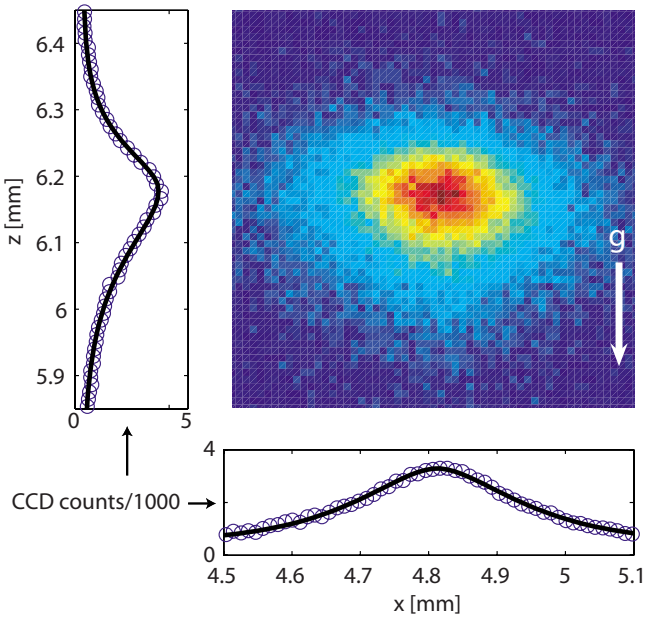

FIG. 4. (Color online) CCD image of magnetically trapped atoms after 0.3 s in the magnetic trap. The marginal distributions and fits to $p_x(x)$ and $p_z(z)$ are shown at bottom and left, respectively. For this image, the fit parameters are $\bar{x}=150$ μm, $\bar{z}=105$ μm, and $\bar{g}=0.23$, corresponding to an effective magnetic moment $\bar{\mu}=3.9\mu_B$ and temperature $T=44\pm7$ μK.

III. MAGNETIC TRAPPING

We now consider the fraction of ground-state atoms that remain magnetically trapped after the MOT beams have been turned off. Assuming these atoms can be described by an effective magnetic moment $\bar{\mu}\geqslant 0$, then the potential energy for a trapped atom is given by

$$U(x,y,z)=\bar{\mu}\sqrt{dB_x^2x^2+dB_y^2y^2+dB_z^2z^2}+Mgz,$$

where M is the atomic mass and g is the gravitational acceleration. In equilibrium at temperature T, the marginal distributions of atoms along the x and z directions are found to be

$$p_x(x)=N_x\exp\left(-2\frac{|x|}{\bar{x}}\sqrt{1-\bar{g}^2}\right)\left(1+2\frac{|x|}{\bar{x}}\sqrt{1-\bar{g}^2}\right),$$

$$p_z(z)=N_z\exp\left(-2\frac{|z|}{\bar{z}}-2\bar{g}\frac{z}{\bar{z}}\right)\left(1+2\frac{|z|}{\bar{z}}\right),$$

where N_x and N_z are normalization constants. The length scales and effects of gravity are characterized by $\bar{g}=Mg/(\bar{\mu}dB_z)$ and $\bar{x}=2k_BT/(\bar{\mu}dB_x)$ with a similar expression for $\bar{z}$. Such a trap is stable against gravity only if $\bar{g}<1$. For $\bar{g}=0$, $\bar{x}$ and $\bar{z}$ are the standard deviations of the cloud, while for $\bar{g}>0$, the cloud stretches along gravity. We capture images of magnetically trapped atomic clouds by loading the MOT for 2 s then extinguishing the loading and trapping lasers, leaving all magnetic fields unchanged. After a variable hold time Δt, we pulse the MOT beams and

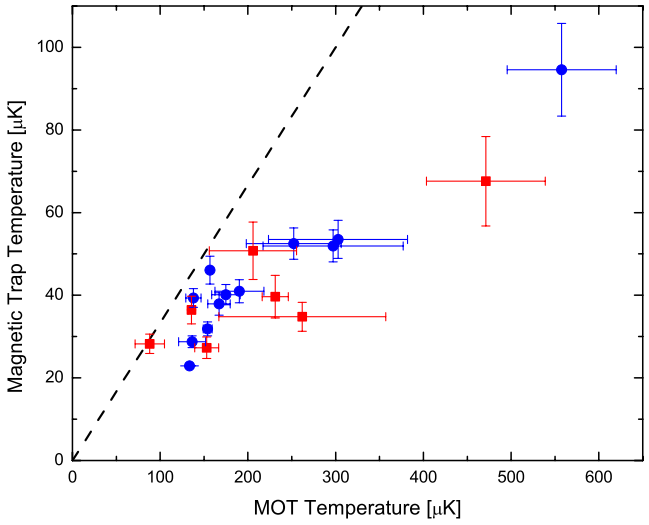

FIG. 5. (Color online) Magnetic trap temperature vs MOT temperature. The MOT temperature was varied by changing the detuning δ. Blue circles and red squares represent data from separate experimental runs at different Zeeman slower and MOT beam intensities. Simple thermodynamic arguments predict that all points should lie above the dashed line where $T_B \geqslant T_M/3$.

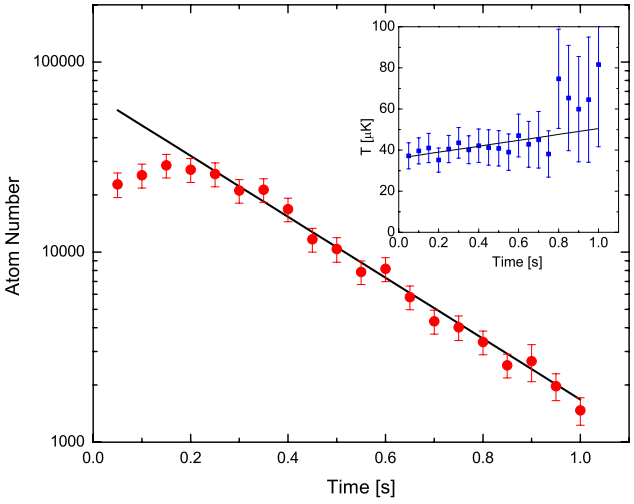

FIG. 6. (Color online) Evolution of the magnetically trapped atom number. After a time $\Delta t \approx 0.2$ s, all of the metastable atoms have returned to the ground state and the trap decays exponentially with a time constant of 270±13 ms (solid line). (Inset) The temperature of the trapped atoms increases over time with an error-weighted heating rate of 14±4 μK/s (solid line).

capture theresulting fluorescence image. Such an image is shown in Fig. 4. By analyzing these images, we can determine T, $\bar{\mu}$, and atom number as the magnetic trap evolves in time [27].

If the magnetic trap loading efficiency is independent of an atom's energy, then thermodynamic arguments [23] predict that the magnetically trapped atom temperature T_B should be related to the MOT temperature T_M by $T_B \geqslant T_M/3$ (equality holds when the spatial extent of the MOT is much smaller than that of the magnetic trap). However, our magnetic trap temperatures systematically violate this bound as shown in Fig. 5, where we measure temperatures below 25 μK. Similar anomalously low temperatures have been observed in MOT-loaded, magnetically trapped Ca [24] and Sr [25] while unexpectedly high temperatures were reported in Cr [23]. In Ref. [25], a selection effect during trap loading was suggested to explain the low temperatures. We suspect a similar phenomenon is at work here, in which spatially dependent optical pumping in the MOT tends to correlate an atom's spin state with its energy; the ejection of atoms in untrapped magnetic states ($m_J \leqslant 0$) may then reduce the average energy of the sample when the MOT is turned off. This hypothesis cannot be quantitatively evaluated without studying the loading efficiency of the magnetic trap, which is difficult to assess due to the presence of trapped, dark-state atoms that cannot be probed directly.

An example of the time evolution of the magnetic trap population and temperature is shown in Fig. 6. Before $\Delta t \approx 0.2$ s, the trap population appears to increase. This is due to the relaxation of metastable atoms back to the ground electronic state where they are resonant with the probe light (MOT beams). After this time, we see single-exponential decay, most likely arising from collisions with the background gas, with a pressure around 2.3×10^{-6} Pa [28]. This claim is further supported by a strong correlation between background gas pressure and trap lifetime and the similar lifetimes for ^{166}Er and ^{168}Er (data not shown). We do not suspect that the trap decay rate is due to density-dependent collisional effects within the trap, because the number densities in the present measurements are not particularly large [we observe peak densities of $n=(2.1\pm0.3) \times 10^9$ cm^{-3}] and because we see no evidence of nonexponential decay. On the other hand, we do not know the origin of the observed heating rate, which may arise from dipolar relaxation processes or collisional heating mechanisms. Improvements to the vacuum system should eliminate our dominant loss channel and allow us to study other relaxation processes. Finally, our data indicate a phase-space density $\rho \approx 2.5 \times 10^{-8}$. It should be straightforward to increase this by at least an order of magnitude by increasing the atomic beam flux.

IV. CONCLUSIONS

In summary, we have presented a number of favorable cooling and trapping properties for atomic erbium. We showed that efficient sub-Doppler cooling occurs in our MOT without the need for an additional optical molasses cooling stage. Furthermore, sub-Doppler cooling should remain effective in large magnetic fields due to the near degeneracy of Landé g factors. This phenomenon may have interesting applications for laser cooling in large magnetic gradient traps, and might be useful for constructing atomic waveguides along magnetic field lines. We also studied the

thermodynamics of a continuously loaded magnetic trap, where temperatures reach unexpectedly low values. The efficient cooling and trapping methods discussed here should be straightforwardly useful as a starting point for phase-space compression towards quantum degeneracy. However, magnetic and collisional relaxation processes must be studied before such a procedure can be considered.

ACKNOWLEDGMENTS

The authors gratefully acknowledge J. L. Hanssen, N. Lundblad, and J. V. Porto for stimulating discussions and D. Rutter and A. Band for technical assistance. S.L. acknowledges support from NIST and NSF. A.B. received financial support from the National Research Council.

[1] M. Takamoto and H. Katori, Phys. Rev. Lett. **91**, 223001 (2003).
[2] M. M. Boyd, T. Zelevinsky, A. D. Ludlow, S. M. Foreman, S. Blatt, T. Ido, and J. Ye, Science **314**, 1430 (2006).
[3] S. G. Porsev, A. Derevianko, and E. N. Fortson, Phys. Rev. A **69**, 021403(R) (2004).
[4] C. W. Hoyt, Z. W. Barber, C. W. Oates, T. M. Fortier, S. A. Diddams, and L. Hollberg, Phys. Rev. Lett. **95**, 083003 (2005).
[5] Y. Takasu, K. Maki, K. Komori, T. Takano, K. Honda, M. Kumakura, T. Yabuzaki, and Y. Takahashi, Phys. Rev. Lett. **91**, 040404 (2003).
[6] T. Fukuhara, Y. Takasu, M. Kumakura, and Y. Takahashi, Phys. Rev. Lett. **98**, 030401 (2007).
[7] J. R. Guest, N. D. Scielzo, I. Ahmad, K. Bailey, J. P. Greene, R. J. Holt, Z. T. Lu, T. P. O'Connor, and D. H. Potterveld, Phys. Rev. Lett. **98**, 093001 (2007).
[8] A. Griesmaier, J. Werner, S. Hensler, J. Stuhler, and T. Pfau, Phys. Rev. Lett. **94**, 160401 (2005).
[9] J. J. McClelland and J. L. Hanssen, Phys. Rev. Lett. **96**, 143005 (2006).
[10] W. C. Martin, R. Zalubas, and L. Hagan, *Atomic Energy Levels—The Rare-Earth Elements* (NSRDS-NBS, Washington: National Bureau of Standards, U.S. Department of Commerce, 1978).
[11] H. Y. Ban, M. Jacka, J. L. Hanssen, J. Reader, and J. J. McClelland, Opt. Express **13**, 3185 (2005).
[12] J. J. McClelland, Phys. Rev. A **73**, 064502 (2006).
[13] C. I. Hancox, S. C. Doret, M. T. Hummon, L. Luo, and J. M. Doyle, Nature (London) **431**, 281 (2004).
[14] J. L. Hanssen, J. J. McClelland, E. A. Dakin, and M. Jacka, Phys. Rev. A **74**, 063416 (2006).
[15] J. H. Wesenberg, K. Molmer, L. Rippe, and S. Kroll, Phys. Rev. A **75**, 012304 (2007).
[16] T. E. Barrett, S. W. Dapore-Schwartz, M. D. Ray, and G. P. Lafyatis, Phys. Rev. Lett. **67**, 3483 (1991).
[17] H. J. Metcalf and P. van der Straten, *Laser Cooling and Trapping* (Springer, New York, 1999).
[18] M. Drewsen, Ph. Laurent, A. Nadir, G. Santarelli, A. Clairon, Y. Castin, D. Grison, and C. Salomon, Appl. Phys. B **59**, 283 (1994).
[19] X. Xu, T. H. Loftus, J. W. Dunn, C. H. Greene, J. L. Hall, A. Gallagher, and J. Ye, Phys. Rev. Lett. **90**, 193002 (2003).
[20] M. Walhout, J. Dalibard, S. L. Rolston, and W. D. Phillips, J. Opt. Soc. Am. B **9**, 1997 (1992).
[21] J. Werner, H. Wallis, and W. Ertmer, Opt. Commun. **94**, 525 (1992).
[22] M. Walhout, U. Sterr, and S. L. Rolston, Phys. Rev. A **54**, 2275 (1996).
[23] J. Stuhler, P. O. Schmidt, S. Hensler, J. Werner, J. Mlynek, and T. Pfau, Phys. Rev. A **64**, 031405(R) (2001).
[24] D. P. Hansen, J. R. Mohr, and A. Hemmerich, Phys. Rev. A **67**, 021401(R) (2003).
[25] S. B. Nagel, C. E. Simien, S. Laha, P. Gupta, V. S. Ashoka, and T. C. Killian, Phys. Rev. A **67**, 011401(R) (2003).
[26] Unless otherwise noted, all uncertainties represent one standard deviation combined random and systematic uncertainty.
[27] In our image analysis, we do not account for Zeeman shifts over the spatial extent of the cloud, which are expected to alter the excited state fraction by at most 7%.
[28] We find good fits to the magnetic trap relaxation data of Fig. 6 for a simple model in which a fraction f of initially dark (metastable) atoms relaxes to the ground state exponentially while atoms are simultaneously lost from the trap at a second exponential rate. However, this larger number of fit parameters cannot give an independent indication of both the initial dark state fraction and the metastable relaxation rate so we have only included a fit to the long-time relaxation behavior here.